Atmospheric nitrous oxide observations above the oceanic surface during CHINARE-18*

ZHU Renbin, SUN Liguang** and LIU Xiaodong

(Institute of Polar Environment, University of Science and Technology of China, Hefei 230026, China)

Received January 3, 2003; revised March 10, 2003

Abstract The gas samples in the marine boundary layer were collected from the track for research ship Xuelong during the 18th Chinese Antarctic Research Expedition (CHINARE-18) and nitrous oxide measurements were made by HP5890ECD-GC in the laboratory. The results represent the shipboard N_2O data set obtained within the lower troposphere with the average concentration of (313.5 ± 2.6)nL·L^{-1} from 31°N to 69°S. The results showed a latitudinally weighted, mean interhemispheric difference of 0.61 nL·L^{-1}. The latitudinal distribution of atmospheric N_2O concentration was analyzed from northern midlatitudes to Southern Ocean around the Antarctic continent and it was showed that N_2O concentration in the current confluences was higher than that in other oceanic areas. This indicated that strong N_2O emissions occurred there. The longitudinal distribution of N_2O concentrations in the Southern Ocean also showed similar situation. According to the interhemispheric difference of atmospheric N_2O concentrations and the two-box model, we estimated that 2/5 of the global flux of N_2O into the atmosphere is derived from the sources in the southern hemisphere.

Keywords: Antarctica, the Pacific Ocean, nitrous oxide, vacuum vial.

Nitrous oxide (N_2O) is one of the most important greenhouse gases, and it plays an important role in the depletion of stratospheric ozone[1]. The atmospheric N_2O concentration has been increasing at the rate of 0.2%~0.3% per year and the global average N_2O concentration has reached 314 nL·L^{-1} [2]. Such a concentration increase is generally ascribed to direct emissions of N_2O to the atmosphere through fertilizer production, crop production, fossil fuel combustion, biomass burning, nitric acid production and sewage, as well as to enhancement of biogenic N_2O emissions by additional fixation of nitrogen by cultivation of leguminous plants and deposition of anthropogenic nitrogen compounds through the atmosphere[3~5]. However, the oceans are also considered significant among the sources of atmospheric N_2O. McElroy and Wofsy calculated the oceanic contribution to be about 13% of all sources[6]. Cohen and Gordon estimated oceanic N_2O concentration arrived at a mean supersaturation of 9%[7]. At the other extreme, Elkins and Singh et al. reported mean saturation anomalies of 25% and 34%[8,9]. Those investigations yielding higher supersaturation focused on equatorial or upwelled waters, and almost all were conducted over a short period and in a relatively small latitudinal range. As a result, the spatial distribution of N_2O in the marine boundary layer over a larger portion of the world's oceans has yet to be understood. Analyses of temporal trend in global N_2O concentration indicate that there has been considerable variation at the rate of increase in N_2O and that this trend seems to be escalating in recent years[10]. Data from ship and ground-based measurements have documented an interhemispheric concentration gradient of 0.2 to 1.0 nL·L^{-1} [11,12]. At this point there remain unanswered questions about the sources of atmospheric N_2O, including a lack of accurate source strengths and some uncertainty in stratospheric loss rates[13]. Therefore it is necessary that atmospheric N_2O concentration be measured in the marine boundary layer over a larger portion of the world's oceans.

During the 18th Chinese Antarctic Research Expedition (CHINARE-18), we collected gas samples in the marine boundary layer from the track for research ship *Xuelong* and analyzed atmospheric N_2O concentration in the laboratory. The latitudes covered the range from 31°N to 69°S. The purposes of this study were (1) to measure the latitudinal or longitudinal variations of atmospheric N_2O in the marine boundary layer, (2) to find out the main environmental factors affecting the concentrations, and (3)

* Supported by Knowledge Innovation Project of CAS (Grant No. KZCX2-302) and the National Natural Science Foundation of China (Grant No. 40076032)

** To whom correspondence should be addressed. E-mail: slg@ustc.edu.cn

to discuss the source strength from the southern hemisphere.

1 Expeditionary areas and methods

The research ship *Xuelong* set out from Shanghai harbor in China on November 15, 2001. Main research and sampling areas included South China Sea, Philippine Sea, Western Pacific and Southern Oceans around Antarctic continent. Research ship *Xuelong* reached the Great Wall Station in Western Antarctica on December 17, 2001 via New Zealand, left this station on December 26, 2001, headed east along the 62°S and reached Zhongshan Station located in Eastern Antarctica on January 16, 2002. Fig. 1 illustrates the ship track from Shanghai harbor to Zhongshan Station.

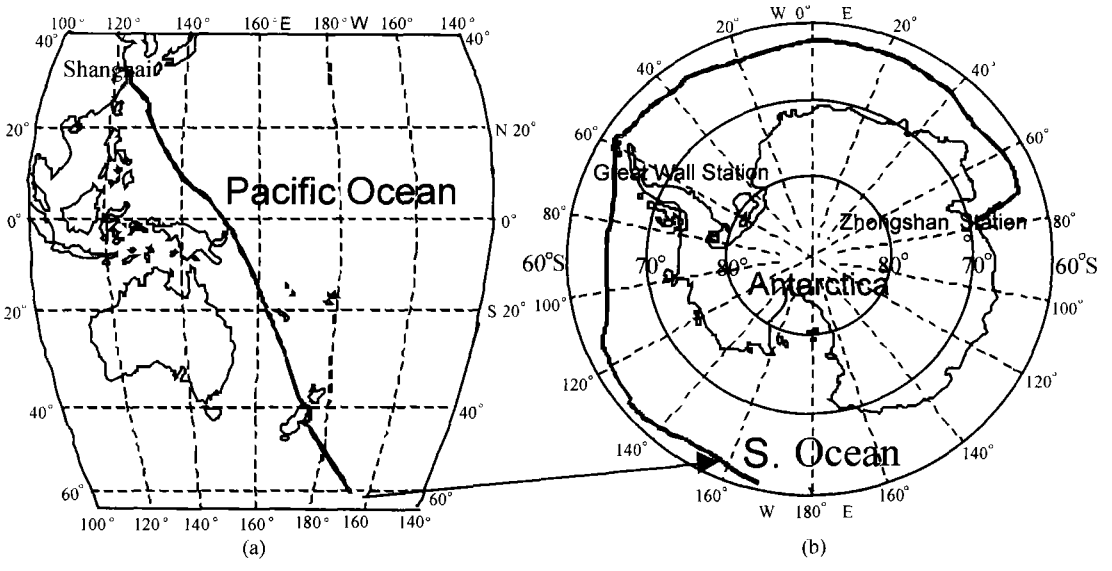

Fig. 1. Track of research ship *Xuelong* from Shanghai to Zhongshan station during the CHINARE-18. The bold line indicates the track of research ship: (a) Western Pacific Ocean and part of Southern Pacific Ocean; (b) the Southern Ocean around the Antarctic continent.

We used vacuum vials (17.5 mL) made in the Institute of Japanese Agricultural Environment, which had been vacuumized to -1.0×10^5 Pa in advance, to collect atmospheric samples above oceanic surface on the track. The sampling height was about 2 m from the deck of the fore. To avoid the impacts of anthropogenic factors and research ship self, we collected gas samples upwind on the fore. Two duplicate gas samples were collected every time to ensure the determination accuracy and sampling time was 8:30 A. M. and 16:30 P. M. (local time) every day, respectively. The air temperature, air pressure, wind direction and its velocity above the oceanic surface were simultaneously recorded to investigate the effects of these climatic factors on the distribution of N_2O concentration. About 300 gas samples in the marine boundary layer were collected on the track. These vials were sealed with a butyl rubber septum and then covered by a plastic cap. High vacuum of -1.0×10^5 Pa inside the vial can remain for one year at least[3,4]. In addition, standard gas stored in the vials also showed no significant change in concentration during the storage in the laboratory or during transportation from the cruise of the research ship (about 140 days), suggesting that the quality of sample air in the vials did not change during the sampling and transport period either[14].

The collected gas samples were brought back to China and analyzed in the laboratory of Material Cycling in Pedosphere, Institute of Soil Science, Chinese Academy of Sciences, for N_2O concentration. N_2O mixing ratios were determined by HP5890 GC using a ^{63}Ni electron capture detector (ECD)[4,14]. GC-ECD was equipped with a back flush system with 10-port valves. A pre-column (2 m) and a main-column (Porapak Q, 100 mesh) were used with an argon-methane (95%: 5%) mixture as the carrier gas at a flow rate of 30 mL·min^{-1}. The detector and column temperatures were 330 ℃ and 85 ℃, respectively. The back flush time was 2.8 min. The injecting gas volume was 3.0 mL, by using an adjustable pressure syringe injector. Compressed air was used as the standard gas with the value of 303 nL·L^{-1} demarcated by the National Institute of Japanese Agricultural

Environment. The variance coefficient for standard samples was within 0.1%～0.4% in ten hours.

2 Results

2.1 The latitudinal distribution of atmospheric N_2O concentration

N_2O data were collected between 31°N and 69°S latitudes and a latitude profile of the lower troposphere data is shown in Fig. 2. The mean N_2O mixing ratio was about $(313.5 \pm 2.6)nL \cdot L^{-1}$. The latitude range near 31°N contained slightly higher N_2O mixing ratios. These observations were performed close to land where the main winds were west to east, and the sampled air mass was significantly influenced by Asian continental sources. The latitude range between 10° N and 10° S clearly contained enhanced N_2O. This latitude range was located in the equatorial warm current (EWC) and countercurrent (ECC) confluence. Previous investigations showed that dissolved N_2O in surface water was elevated near the equator and at 10°S, which may be associated with upwelling that occurred near the boundary of the ECC and EWC[8,9]. Some investigators reported the anomalous supersaturation of 20%, 34% and 37% for the major upwelling regions[8,9,12]. The high N_2O mixing ratios in this latitude range probably resulted from the strong emissions from surface water, which was related with the upwelling that occurred near the equator. A larger variation of N_2O concentrations appeared near 5°S, which may be related with anthropogenic sources since the track was close to the land. The highest mixing ratios were noted between 40° S and 50°S latitudes, which may have reflected a great continental influence since the track ran closer to New Zealand. In addition, elevated atmospheric N_2O in this oceanic area may be related with upwelling that occurred near the boundary of Australian warm current (AWC) and strong westerly flows. These were the highest atmospheric concentrations observed during the entire trip with the mean value of $(316.6 \pm 4.7)nL \cdot L^{-1}$. Furthermore elevated atmospheric N_2O mixing ratios were also noted in the higher south latitudes, which were located in the confluence of coast cooling current (CCC) around Antarctica and westerly flow.

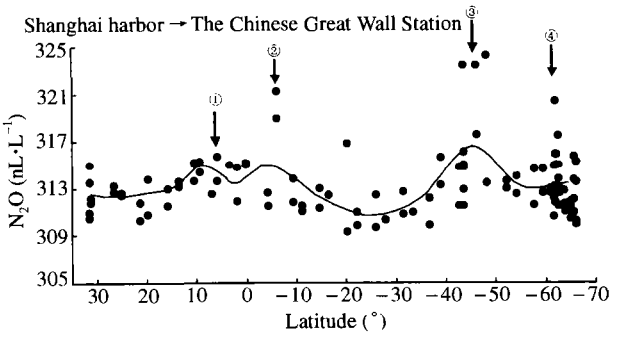

Fig. 2. The latitudinal distributions of atmospheric N_2O concentration on the track of the research ship. The positive and negative values indicate northern and southern latitudes, respectively. The arrows and numbers indicate the current confluences and their marks, respectively (the same as Table 1). The average curve is also drawn in the figure.

On the other hand, the latitude ranges located in the equatorial warm currents (EWC) showed a slight decrease in the N_2O mixing ratio, which may be related with low N_2O fluxes from the surface water in the oceanic regions since dissolved N_2O in surface water was saturated to slightly undersaturated according to the observations by Butler et al.[12] The lowest mixing ratios were observed in the latitude range between 20° S and 30° S which were almost not influenced by oceanic currents, little emissions occurred there and atmospheric N_2O was almost equilibrium with the dissolved N_2O in surface water[12]. According to the analyses above, the distribution of atmospheric N_2O at the track of research ship was related with the oceanic currents. Higher N_2O mixing ratios occurred in the current confluences, suggesting that these oceanic areas are strong atmospheric N_2O sources. Atmospheric N_2O mixing ratio and oceanic current at different latitudes are listed in Table 1. From Table 1, mean N_2O concentrations above the oceanic surface were slightly higher than those obtained at Chinese atmospheric observation stations and Antarctic Fildes Peninsula[15].

Table 1. The relationship between atmospheric N_2O mixing ratio and oceanic current in the different latitude ranges on the track of the research ship

Range	Average N_2O ($nL \cdot L^{-1}$)	s.d ($nL \cdot L^{-1}$)	Oceanic currents
31°N～20°N	312.3	1.3	The branch of northern equatorial warm current.
20°N～10°N	313.1	1.4	Northern equatorial warm current.
10°N～0°N	314.2	1.3	The confluence of northern equatorial warm current and equatorial countercurrent. ①
0°S～10°S	315.0	4.1	The confluence of equatorial countercurrent and southern equatorial warm current. ②
10°S～20°S	312.2	2.3	Southern equatorial warm current.
20°S～30°S	310.7	1.1	
30°S～40°S	312.2	1.9	

To be continued

Continued

Range	Average N_2O ($nL \cdot L^{-1}$)	s.d. ($nL \cdot L^{-1}$)	Oceanic currents
40°S~50°S	316.6	4.7	The confluence of Australian warm current and westerly flows. ③
50°S~60°S	313.2	1.0	Westerly flows.
60°S~69°S	313.4	2.3	The confluence of cool current around Antarctica and westerly flows. ④
Fildes Peninsula	311.4	2.6	
Linan Station[15]	309.0	4.6	
Longfeng Mountain[15]	311.0	4.5	
Waliguan Station[15]	310.8	3.0	

Note: the data for oceanic currents are from the pamphlet for World Map (Hunan Map Press, 2001)

2.2 The longitudinal distribution of N_2O concentration in the Southern Ocean

Over the expanse of the Southern Ocean around the Antarctic continent the N_2O levels containing only data between 63° and 69° S latitudes are shown in Fig. 3. A selected band of latitudes was chosen so that any latitude bias would be removed and these particular latitudes were selected solely because this range of latitudes contains N_2O observations across a significant longitude range (180°W ~ 80°E). Atmospheric N_2O mixing ratio fluctuated at the value of 313.0 $nL \cdot L^{-1}$ and the mean concentration was $(313.4 \pm 2.2) nL \cdot L^{-1}$. Three peaks appeared in the longitude ranges of 180° ~ 130°W, 50°W ~ 10°E and 65° ~ 80°E, respectively. These longitude ranges are located near the boundary of westerly flow and coast cool currents around Antarctica (CCC) and high N_2O production and emission may occur there. Other longitudinal ranges are mainly influenced by CCC and lower N_2O emissions occur there.

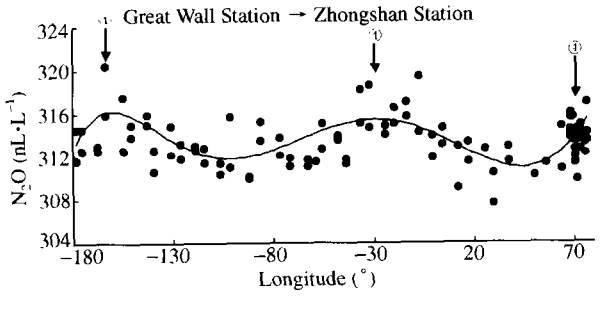

Fig. 3. The longitude distributions of atmospheric N_2O mixing ratios on the track in Southern Ocean. The positive and negative values represent eastern and western longitudes, respectively. The arrows and numbers indicate the current confluences and their marks, respectively (the same as Table 1). The average curve is also drawn in the figure.

3 Discussion

3.1 Interhemispheric concentration gradient

From Fig. 2, we can see an interhemispheric difference of 0.61 $nL \cdot L^{-1}$ between 31° ~ 0°N and 0° ~ 31°S. Since the latitudinal range is close to the central Pacific, the N_2O emission from anthropogenic sources is very low and the values obtained from these samples are closer to the average concentration on the globe. Therefore the concentration difference may reflect the subtle interhemispheric tropospheric N_2O gradient. Early data from studies were imprecise and precluded the detection of a subtle tropospheric gradient[16]. However, the measurement and calibration of atmospheric N_2O have improved considerably in the past decade. Random and systematic errors have been reduced[17]. Thus data from various investigations now are highly precise and much more comparable than those in previous decades. Weiss reported that interhemispheric N_2O concentration difference did not appear constantly, ranging from 0.5 ~ 1.0 $nL \cdot L^{-1}$ [11]. Khalil et al. suggested the measurable variations in the interhemispheric difference might be explained by seasonal variations in atmospheric N_2O[18]. The difference would be the largest during the northern hemispheric spring and early summer and the smallest during the northern hemispheric fall and winter. For example, the lowest value reported, 0.2 $nL \cdot L^{-1}$, is for measurements made in January of each year[19]. Our value of 0.61 $nL \cdot L^{-1}$ was obtained from measurements taken during the northern hemispheric winter and was almost consistent with other observations considering the seasonal variations[11,18,19].

3.2 Estimate of relative hemispheric source strengths of N_2O

Relative source strengths of N_2O in the two hemispheres can be estimated from the atmospheric accumulation rate and the latitudinal gradient. For a first-order approximation, we have chosen an approach similar to that of Butler et al.[12] and Khalil et al.[18]. In this two-box model, the change in concentration of N_2O in each hemisphere can be represented by the following mass-balance equations:

$$M_n\left(\frac{dC_n}{dt}\right) = P_n - \frac{M_n C_n}{\tau} - \frac{M_n(C_n - C_s)}{\tau_e}, \quad (1)$$

$$M_s\left(\frac{dC_s}{dt}\right) = P_s - \frac{M_s C_s}{\tau} + \frac{M_n(C_n - C_s)}{\tau_e}, \quad (2)$$

where dc/dt is the growth rate, M the total atmospheric mass in each hemisphere, P the source

strength in each hemisphere, τ the atmospheric lifetime, τ_e interhemispheric exchange time, and the subscripts n and s refer to the northern and southern hemisphere. The relative source strength $\gamma = P_n/P_s$ follows from (1) and (2). If we let the difference in hemispheric concentration $\Delta C_{ns} = C_n - C_s$ and assume that the total tropospheric mass of the two hemispheres is equal and that $dC_n/dt = dC_s/dt = b$, then the relative source strength becomes

$$\gamma = \frac{\tau(\tau_e b + \Delta c_{ns}) + \tau_e C_n}{\tau(\tau_e b - \Delta c_{ns}) + \tau_e C_s}. \quad (3)$$

Finally, we have chosen to express our results as the relative strength of southern hemispheric sources, R_s, where

$$R_s = \frac{P_s}{P_n + P_s} = \frac{1}{1+\gamma}. \quad (4)$$

Using the value of 1.1 years for τ_e reported by Butler et al.[12] and considering that τ is 100 to 150 years, and that annual growth rates range from 0.66 to 1.0 $nL \cdot L^{-1}$ in each hemisphere[12,17], we calculated R_s based upon the interhemispheric difference in concentration. The results show a relatively large range for R_s. To sustain an interhemispheric gradient of 0.5~0.7 $nL \cdot L^{-1} \cdot yr^{-1}$, the southern hemisphere would have to supply over 2/5 of the global flux of N_2O (Table 2). On the other hand, for an interhemispheric gradient of 0.8~1.1 $nL \cdot L^{-1}$, the contribution from the southern hemispheric would be about 1/3 of the total.

Table 2. Relative southern hemispheric flux of N_2O (R_s) (% of total global flux)

$C_n - C_s$(nL/L)	Reference	R_{s1}(%)	R_{s2}(%)
0.50	Weiss (1981)	42~44	42~44
0.61	This study	41~43	40~43
0.77	Weiss (1981)	38~41	37~41
0.97	Butler et al. (1989)	35~39	34~38
1.1	Khalil and Rasmussen (1988)	33~38	31~36

Note: C_n, northern hemisphere mean concentration; C_s, southern hemisphere mean concentration; R_{s1}, $dc/dt = 1.0\ nL \cdot L^{-1} \cdot yr^{-1}$ (Khalil and Rasmussen, 1988); R_{s2}, $dc/dt = 0.66\ nL \cdot L^{-1} \cdot yr^{-1}$ (Butler et al. 1989); $\tau_e = 1.1$ yr. Range of values for R_s is for τ of 150 and 100 years.

4 Conclusions

(i) Atmospheric mean N_2O concentration was about $(313.5 \pm 2.6)\ nL \cdot L^{-1}$ on the track of the research ship *Xuelong* and the interhemispheric N_2O concentration gradient was about 0.61 $nL \cdot L^{-1}$.

(ii) The distribution of atmospheric N_2O concentrations was related with oceanic currents on the track. High N_2O mixing ratios appeared in the current confluences, indicating that strong N_2O emissions occurred there.

(iii) According to our observations, the contribution from the southern hemisphere would be about 2/5 of the globe.

The results in this paper were just obtained from one track of the research ship during CHINARE-18, therefore the conclusions above need to be further justified and further research is also needed.

Acknowledgements We would like to thank Polar Office of National Oceanic Bureau of China and members on the research ship *Xuelong* for their support and assistance.

References

1 Crutzen, P. et al. Effects of nitrogen and combustion on the stratospheric ozone layer. Ambio., 1977, 6: 112.
2 Flückiger, J. et al. Variations in atmospheric N_2O concentration during abrupt climatic changes. Science, 1999, 285: 227.
3 Xing, G. X. N_2O emission from cropland in China. Nutrient Cycle in Agroecosystem. 1998, 52: 249.
4 Xing, G. X. et al. Preliminary studies on N_2O emission fluxes from upland soil and paddy soils in China. Nutrient Cycle in Agroecosystems. 1997, 49: 249.
5 Mosier, A. R. et al. Impaction of agriculture on soil consumption of atmospheric CH_4 and N_2O flux in subarctic, temperate and tropical grasslands. Nutrient Cycling in Agroecosystems, 1997, 49: 71.
6 McElroy, M. B. et al. Tropical forests: Interactions with the atmosphere. In: Tropical Rain Forests and World Atmospheres. Boulder: West View Press, 1986: 33.
7 Cohen, Y. et al. Nitrous oxide production in the ocean. J. Geophys. Res., 1979, 84: 347.
8 Elkins, J. W. et al. Aquatic sources and sinks for nitrous oxide. Nature, 1978, 275: 602.
9 Singh, H. B. et al. The distribution of nitrous oxide (N_2O) in the global atmosphere and the Pacific Ocean. Tellus, 1979, 31(4): 313.
10 Khalil, M. A. K. et al. The global sources of nitrous oxide. J. Geophys. Res., 1992, 97: 14651.
11 Weiss, R. F. The temporal and spatial distribution of tropospheric nitrous oxide. J. Geophys. Res., 1981, 86(C8): 7185.
12 Butler, J. H. et al. Tropospheric and dissolved N_2O of the west Pacific and east Indian Oceans during the El Nino southern oscillation event of 1987. J. Geophys. Res., 1989, 94: 14, 865.
13 IPCC. In: Houghton, J. H. et al. (eds). Climate Change 2001: The Scientific Basis. New York: Cambridge University Press, 2001, 78.
14 Sun, L. G. et al. Emissions of N_2O and CH_4 from Antarctic tundra soil: role of penguin dropping deposition. Atmospheric Environment, 2002, 36(31): 4977.
15 Wang, M. L. et al. Atmospheric N_2O concentrations in Chinese part clean regions. In: Monitoring the Concentrations and Emissions of Greenhouse Gases and Their Related Processes. Beijing: Environment Science Press (in Chinese), 1996, 53.
16 Pierotti, D. et al. The atmospheric distribution of nitrous oxide. J. Geophys. Res., 1977, 82(37): 5823.
17 Khalil, M. A. K. et al. Nitrous oxide: trends and global mass balance over the last 3000 years. Ann. Glaciol., 1988, 10: 73.
18 Khalil, M. A. K. et al. Increase and seasonal cycles of nitrous oxide in the earth's atmosphere. Tellus, 1983, 35B: 161.
19 Rasmussen, R. A. et al. Atmospheric trace gases: trends and distributions over the last decade. Science, 1986, 232: 1623.